



## Giving your work a new shine

The New LCMS-9050 Q-TOF mass spectrometer integrates the world's fastest and most sensitive quadrupole technology with TOF architecture. Facilitate your work and improve your results thanks to trusted mass accuracy stability, ultra-stable polarity switching, highest speed for MS/MS and a great versatility with flexible extensions. Discover all the advantages of the new LCMS-9050 – also available as an upgrade for your LCMS-9030.

**Reduced ambiguity**  
in compound identification and structural elucidation.

**Less effort for instrument management,**  
more time for the real data.

**Increased availability and throughput**  
on the system.

## RESEARCH ARTICLE

# Suitability of different reconstructed human skin models in the skin and liver Chip2 microphysiological model to investigate the kinetics and first-pass skin metabolism of the hair dye, 4-amino-2-hydroxytoluene

Katrin Brandmair<sup>1</sup> | Thi-Phuong Tao<sup>2</sup> | Silke Gerlach<sup>1</sup> | Julia Przibilla<sup>3</sup> |  
 Andreas Schepky<sup>1</sup> | Uwe Marx<sup>2</sup> | Nicola J. Hewitt<sup>4</sup>  | Jochen Kühnl<sup>1</sup> |  
 Ilka Maschmeyer<sup>2</sup>

<sup>1</sup>Beiersdorf AG, Unnastraße 48, D-20253, Hamburg, Germany

<sup>2</sup>TissUse GmbH, Oudenarder Str. 16, D-13347, Berlin, Germany

<sup>3</sup>Pharmacelsus GmbH, Science Park 2, D-66123, Saarbrücken, Germany

<sup>4</sup>Cosmetics Europe, Avenue Hermann-Debroux 40, 1160, Auderghem, Belgium

#### Correspondence

Nicola J. Hewitt, Wingertstrasse 25, 64390 Erzhausen, Germany.

Email: [nickyhewitttd@yahoo.co.uk](mailto:nickyhewitttd@yahoo.co.uk)

#### Funding information

Cosmetics Europe Long Range Science Strategy programme

#### Abstract

The HUMIMIC skin-liver Chip2 microphysiological systems model using the epidermal model, EpiDerm™, was reported previously to mimic application route-dependent metabolism of the hair dye, 4-amino-2-hydroxytoluene (AHT). Therefore, we evaluated the use of alternative skin models—SkinEthic™, EpiDermFT™ and PhenionFT™—for the same purpose. In static incubations, AHT permeation was similar using SkinEthic™ and EpiDerm™ models. Older Day 21 (D21) SkinEthic™ models with a thicker stratum corneum did not exhibit a greater barrier to AHT (overall permeation was the same in D17 and D21 models). All epidermal models metabolised AHT, with the EpiDerm™ exhibiting higher *N*-acetylation than SkinEthic™ models. AHT metabolism by D21 SkinEthic™ models was lower than that by D17 SkinEthic™ and EpiDerm™ models, thus a thicker stratum corneum was associated with fewer viable cells and a lower metabolic activity. AHT permeation was much slower using PhenionFT™ compared to epidermal models and better reflected permeation of AHT through native human skin. This model also extensively metabolised AHT to *N*-acetyl-AHT. After a single topical or systemic application of AHT to Chip2 model with PhenionFT™, medium was analysed for parent and metabolites over 5 days. The first-pass metabolism of AHT was demonstrated, and the introduction of a wash step after 30 min decreased the exposure to AHT and its metabolites by 33% and 40%–43%, respectively. In conclusion, epidermal and FT skin models used in the Chip2 can mimic the first-pass skin metabolism of AHT. This highlights the flexibility of the Chip2 to incorporate different skin models according to the purpose.

Katrin Brandmair and Thi-Phuong Tao, shared first author—contributed equally.

Jochen Kühnl and Ilka Maschmeyer, shared last author—contributed equally.

This is an open access article under the terms of the [Creative Commons Attribution-NonCommercial-NoDerivs](https://creativecommons.org/licenses/by-nc-nd/4.0/) License, which permits use and distribution in any medium, provided the original work is properly cited, the use is non-commercial and no modifications or adaptations are made.

© 2023 The Authors. *Journal of Applied Toxicology* published by John Wiley & Sons Ltd.

## KEYWORDS

4-amino-2-hydroxytoluene, Chip2, cosmetics, EpiDerm, EpiDermFT, first-pass metabolism, microphysiological systems, PhenionFT, skin, skin models

## 1 | INTRODUCTION

Since the European ban on the testing of cosmetic ingredients on animals (EU, 2003), the assessment of the safety of cosmetic ingredients relies on the use of non-animal methods to evaluate their biological effects and link these with systemic concentrations to establish a margin of safety (Alexander-White et al., 2022; Dent et al., 2021; Desprez et al., 2018). Therefore, fit-for-purpose in vitro options are required to determine the metabolic fate and plasma/tissue distribution of an ingredient after application. The main route of exposure to cosmetics ingredients is via the skin; therefore, first-pass metabolism in the skin is relevant to ingredients as they penetrate the viable skin layers (Géniès et al., 2019, 2020), prior to liver metabolism after entering the systemic circulation. The metabolism and distribution kinetics of a compound in the body can be modelled using physiologically based kinetic (PBK) models (Moxon et al., 2020; Ouedraogo et al., 2022). While these previously focussed on oral and parenteral routes of administration, there is increased use of PBK models including a skin module to incorporate the simulation of topically applied compounds (Li et al., 2022; Najjar et al., 2022). However, these models generally do not simulate metabolism in the skin. PBK models also rely on the quality of the in vitro data used as input (Li et al., 2022), which are generated in separate assays. An alternative option to evaluate the direct interaction between skin and liver metabolism in a single assay is to use in vitro microphysiological systems (MPS). These microfluidic devices can connect tissue models (referred to here as 'organoids') via a circuit through which medium is pumped. There are several MPS currently available that include a compartment for a skin model connected to other organs such as the gut (Lee & Sung, 2022) and liver (Kühnl et al., 2021; Tao et al., 2021; Tavares et al., 2020). More recently, the HUMIMIC skin and liver Chip2 model has been adapted to include a third organoid to link the kinetics with the toxicodynamic effect of the test compound. The resulting skin-liver-thyroid Chip3 model has been used to evaluate the potential for topically applied compounds to cause endocrine disruption by altering thyroid hormone production (Tao et al., 2023).

As the cosmetics industry cannot use in vivo animal assays, alternative approaches are required for every endpoint; therefore, MPS could address this need as a partial replacement for the standard in vivo rodent toxicokinetics studies. Our initial proof-of-concept studies focussed on characterising the application scenario-dependent pharmacokinetics and pharmacodynamic properties of model compounds, permethrin and hyperforin (Kühnl et al., 2021). These showed that the measurement of parent and metabolites was reproducible across Chip2 circuits and across two laboratories, highlighting the robustness and transferability of the method. In a second phase of

the project, we evaluated the suitability of the HUMIMIC skin-liver Chip2 model to recapitulate the route-specific metabolism of the hair dye, 4-amino-2-hydroxytoluene (AHT), observed in legacy in vivo rat toxicokinetics studies (Goebel et al., 2009). The three major metabolites of AHT are *N*-acetyl-AHT, AHT-O-sulphate and AHT-O-glucuronide (Goebel et al., 2009). After intravenous or oral administration, *N*-acetyl-AHT represented 37% and 32% of the total metabolites in urine, respectively; however, this increased to 66% when AHT was applied topically. This finding indicates that AHT *N*-acetylation occurred in the skin prior to entering the systemic circulation, that is, a first-pass metabolism effect. In the skin-liver Chip2 model, first-pass skin metabolism was investigated by comparing the concentrations of metabolites after application of AHT to the skin surface with that after adding it to the liver compartment (i.e., the 'systemic route'). Results showed that there was a higher peak concentration and area under the curve (AUC) of *N*-acetyl-AHT in the circuit after topical application compared to systemic application, and a concomitantly lower peak concentration and AUC of AHT-O-sulphate, both of which were in line with in vivo studies in rats. Another aspect in a safety assessment is that the ingredient is whether data can be generated in an experiment, which reflects human consumer exposure. For example, when AHT and other hair dyes are used, they are typically removed from the skin after 30 min. Tao et al. (2021) demonstrated how the Chip2 model could be used to represent this consumer-relevant exposure by rinsing AHT from the skin and then monitoring the presence of AHT and its metabolites in the chip circuit. The result showed that rinsing the skin after 30 min markedly decreased the internal exposure (in the Chip2 circuit) to AHT and its metabolites.

During the studies with AHT, it was noted that the permeation of AHT through the EpiDerm™ models used in the Chip2 model was faster than in native human skin (Goebel et al., 2009). The shorter residence time of AHT in the skin model was associated with a low ratio of first pass metabolism at higher AHT concentrations due to saturation of the NAT enzymes in EpiDerm™ models at doses of ~2.5 μM and higher. Because the Chip2 model can be equipped with different skin models, we evaluated other skin models for their suitability to reflect the permeation and metabolism of AHT observed in native human skin. These included the epidermal model, SkinEthic™, and the full-thickness (FT) models, EpiDermFT™ and PhenionFT™. Results for static and skin-liver Chip2 incubations for the EpiDerm™ model and skin-liver Chip2 incubations for the EpiDermFT™ model have been published by Tao et al. (2021). Here, we have measured the permeation and metabolism of AHT in static incubations with SkinEthic™ and PhenionFT™ skin models and in the skin-liver Chip2 using PhenionFT™ models. The PhenionFT™ model was also used to

demonstrate the effect of washing the PhenionFT™ surface after 30 min on AHT concentrations and metabolites present in the circuit. The results from the current study were compared with those reported by Tao et al. (2021) using EpiDermFT™ and PhenionFT™.

## 2 | MATERIALS AND METHODS

### 2.1 | Chemicals

AHT, product number A0925, was from Tokyo Chemical Industry CO, LTD Eschborn, Germany. *N*-(3-Hydroxy-4-methylphenyl)acetamide (*N*-acetyl-AHT), 5-amino-2-methylphenyl hydrogen sulphate (AHT-O-sulphate), AHT-O-glucuronide and 5-acetamido-2-methylphenyl hydrogen sulphate (*N*-acetyl-AHT-O-sulphate) were from SpiroChem AG, Basel, Switzerland. All chemicals were of the highest purity.

### 2.2 | Skin models and media

PhenionFT™ (FT SMALL-1), 24-well format were purchased from Henkel AG & Co. KGaA, 40191 Düsseldorf, Germany. The associated medium was Air Liquid Interface Culture Medium (ALI CM PR\*-250). The SkinEthic™ RHE model, 96-well format was a gift from EPISKIN, 69366 LYON, France. The associated medium was Maintenance medium.

### 2.3 | Static incubations with PhenionFT™ and SkinEthic™ skin models

The permeation and metabolism of AHT was measured in 24-well PhenionFT™ and 96-well SkinEthic™ RHE models according to the method described by Tao et al. (2021) for EpiDerm™ models. Two different 'ages' of SkinEthic™ RHE models were tested. The first was a 'Day 17' model, which were used 1 day after delivery, as recommended by the supplier. The second was a 'Day 21' model, which was used after a 5-day pre-culture to allow the thickening of the stratum corneum. The reason for using models with a thicker stratum corneum was to determine whether this resulted in a greater barrier to hydrophilic compounds, for example, AHT.

Skin models were transferred to fresh 24- or 96-well plate (depending on the size of the model) containing 0.2 mL (SkinEthic™ models, 0.11 cm<sup>2</sup> surface area) or 0.5 mL (PhenionFT™ models, 0.6 cm<sup>2</sup> surface area) of the associated medium and incubated at 37°C and 5% CO<sub>2</sub> for 1 h prior to the incubations. A volume of the AHT working solution was applied to the top of the skin model (2 µL to SkinEthic™ models and 10 µL to PhenionFT™ models) so that the volume per cm<sup>2</sup> were similar (18.2 µL/cm<sup>2</sup> for SkinEthic™ models and 16.6 µL/cm<sup>2</sup> for PhenionFT™ models). The resulting doses were equivalent to a calculated final concentration of 2.5 µM in the medium below based on a 100% permeation at 37°C (triplicates). Skin models were incubated for up to 2 h after topical application of AHT. Sampling of different timepoints was conducted by transferring the

models into new wells containing fresh medium while the 'used' medium was collected for parent/metabolite analysis.

### 2.4 | Liver spheroid preparation for Chip2 incubations

Liver spheroids were generated according to the method described by Tao et al. (2021). Differentiated HepaRG cells (HPR116) were obtained from Biopredic International (Rennes, France), cryopreserved human stellate cells were from Provitro (Berlin, Germany), and stellate cell medium was from Provitro. At the start of the Chip2 experiment, 40 spheroids were placed into the liver culture compartment of the Chip2.

### 2.5 | Chip2 experiments with liver and PhenionFT™ skin models

Chip2 circuits were equilibrated with a 50:50 mix of HepaRG medium and ALI CM PR\*-250 medium at least 1 day prior to the start of the experiment. On Day -1 (i.e. 1 day before treatment), 40 liver spheroids were transferred to one compartment of the Chip2, while one skin model in a Millicell culture insert was integrated into the second culture compartment. The circuit was filled with 500 µL fresh medium. The Chip2 circuits were connected to HUMIMIC Starter, the pump control units, operating at a pressure of 350 mbar and vacuum of 300 mbar with 0.5 Hz as the pump frequency. The chips were only removed from the Starter during medium exchange.

One day after inoculation of the Chip2 with the skin models and liver spheroids (Day 0), the exposure to AHT (or solvent control) was started by a single topical or systemic application of AHT (or ethanol as the solvent control). AHT was dissolved in ethanol and further diluted to obtain the working solutions for systemic and topical applications (0.625 and 0.125 mM, respectively). For systemic application, 2 µL of the AHT 0.625 mM working solution (or ethanol) were mixed into 250 µL medium, which was added to the liver compartment after removal of 250 µL medium (resulting in a final concentration of 2.5 µM in the Chip2). For topical application, 10 µL of the 0.125 mM working solution was applied to the top of the skin model (i.e., a topical dose of 16.6 µL/cm<sup>2</sup>, to result in a hypothetical maximum final concentration of 2.5 µM in the Chip2, based on 100% skin absorption). The larger skin model format also required a larger insert in the Chip2 model to accommodate the skin cell culture insert; however, the circuit volume was the same (500 µL). After a single topical application, the AHT either remained on the skin for the duration of the assay ('leave-on') or was washed off the skin surface after 30 min ('rinse-off'). The washing process involved six iterative cycles of careful application and removal of 0.5 mL PBS to and from the skin surface using a pipette (this was based on the method used by Tao et al. [2021], which was shown previously to be effective in removing all the AHT from the surface of the EdiDerm™ models, i.e., the concentration of AHT in the sixth wash was below the lower limit of

quantification [LLOQ]). The skin wash media were collected and analysed for the presence of AHT and *N*-acetyl-AHT.

For metabolite analysis only, samples of medium were removed after 1 and 4 h (from separate circuits per timepoint such that only 80  $\mu$ L was removed from each). At 24 h (Day 1), a volume of 170  $\mu$ L medium was removed from the circuits and replaced with 250  $\mu$ L of fresh medium (without AHT or ethanol), and then every 24 h, a volume of 250  $\mu$ L medium was removed from the circuits and replaced with 250  $\mu$ L of fresh medium (without AHT or ethanol). A volume of 80  $\mu$ L of the sampled medium was aliquoted into 1.5 mL tubes or 96-well plates and stored at  $-80^{\circ}\text{C}$  until analysis by LC-MS/MS. All remaining supernatants were transferred into 96-deep well plates and stored at  $4^{\circ}\text{C}$  until lactate dehydrogenase (LDH), glucose, lactate and albumin analyses were performed. Tissues were harvested after 24, 48 and 120 h to substance exposure from the Chip2 and processed further for histochemical analysis.

## 2.6 | End point measurements employed in static and/or Chip2 experiments

### 2.6.1 | Organoid structure and viability measurements

In Chip2 experiments, the integrity of the skin models was confirmed before application and on Days 1, 2 and 5 by measuring the transepithelial electrical resistance (TEER) using the EVOM2 device with the associated STX2 probe. Additionally, the structures of skin models for all replicate samples in each experiment were monitored using haematoxylin and eosin staining.

Viability end points included: albumin production (Chip2 experiments), glucose consumption (Chip2 experiments), lactate production (Chip2 experiments) and release of LDH (static incubations and Chip2 experiments). Albumin content of the medium was measured using Albumin in Urine/CSF FS Kit from DiaSys (Holzheim, Germany). Lactate concentrations in the medium were measured using the FluitestR Lactate kit from Analyticon (Lichtenfels, Germany). Glucose concentrations in the medium were measured using the Glucose (HK) Kit from Thermo Fisher Diagnostics (Hennigsdorf, Germany). The LDH contents of the medium and lysed skin models and liver spheroids were measured using the LDH (IFCC) Kit from Thermo Fisher Diagnostics.

### 2.6.2 | Quantification of AHT and its metabolites

The quantification of AHT and four of its metabolites was according to the method described by Tao et al. (2021). Samples were prepared by adding 30  $\mu$ L acetonitrile plus internal standards (griseofulvin, diazepam and diclofenac) to 60  $\mu$ L of the standards or samples and mixed vigorously for 10 s. After centrifugation ( $2200 \times g$ , 5 min at room temperature), the supernatant was transferred into vials to LC/MS for quantification. Calibration curves for AHT and its metabolites were

constructed over a concentration range of 1 to 20,000 nM. The specified LLOQ for AHT, *N*-acetyl-AHT, AHT-O-sulphate and AHT-O-glucuronide was 25 nM, and the LLOQ for *N*-acetyl-AHT-O-sulphate was 50 nM.

### 2.6.3 | Statistical analysis and calculations

Statistical analyses were conducted using Prism GraphPad software, Version 6.07 or Microsoft Excel, Version 2003. Statistical differences were evaluated using the paired two-tailed *t*-test, where a statistical difference is denoted when  $p < 0.05$ .

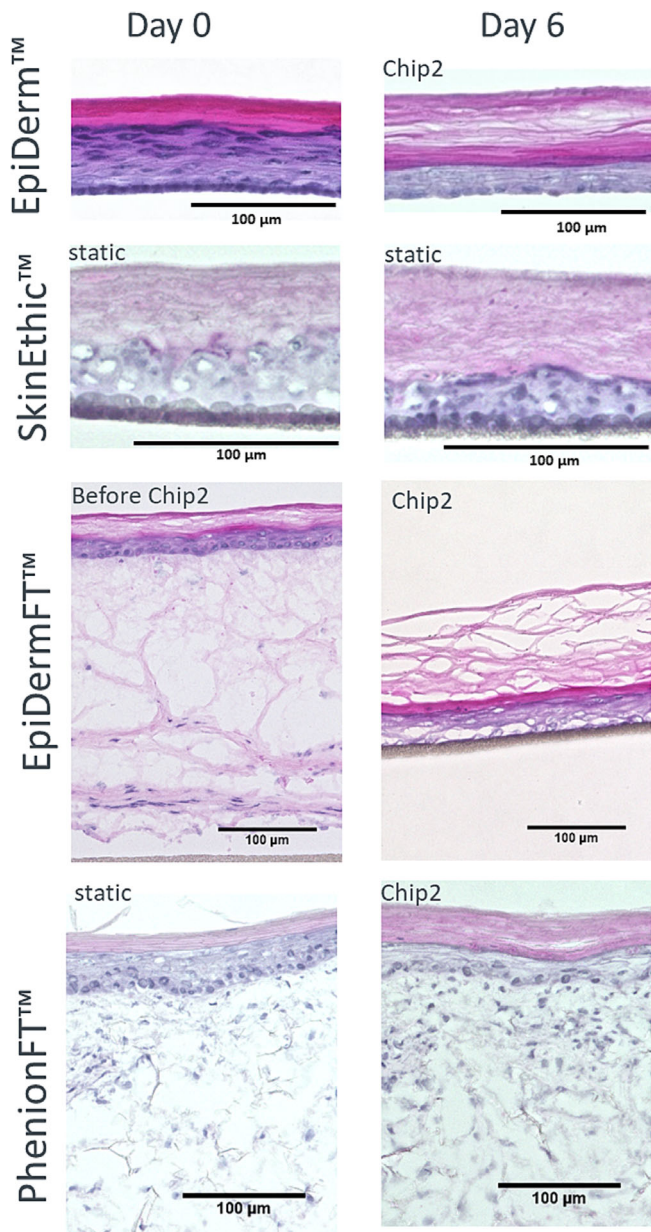
## 3 | RESULTS

### 3.1 | Comparison of skin model morphology

Figure 1 shows the morphology of sections of the skin models tested here, as well as the EpiDerm™ and EpiDermFT™ models used in previous studies for comparison. The EpiDerm™ structure changed over time in the Chip2 model, with a thicker stratum corneum containing large spaces. While the epidermal layer was much thinner, it remained intact (this was reflected in the TEER values, as reported by Tao et al. [2021]). The stratum corneum of the D17 SkinEthic™ model (which was only tested in static incubations) was also thicker after Day 6 and appeared to be more compact than the EpiDerm™ model at the same timepoint. The two FT models exhibited a similar structure to native human skin on Day 0, with a stratum corneum, epidermis and a thick dermis consisting of dense connective tissue and fibroblasts. By Day 6, there was a marked difference in the structures of the FT models in the Chip2 model. The stratum corneum of the EpiDermFT™ model was less compact and the dermis was much thinner compared to Day 0, which was detaching from the insert filter. This model showed signs of early parakeratosis and a basket weave appearance of the stratum corneum and a highly vacuolated sub-basal layer detached from the basal lamina. By contrast, the thickness of the layers in the PhenionFT™ models remained the same over the time course of the incubations (with some vacuoles near the basement membrane, dyskeratosis and a looser dermis).

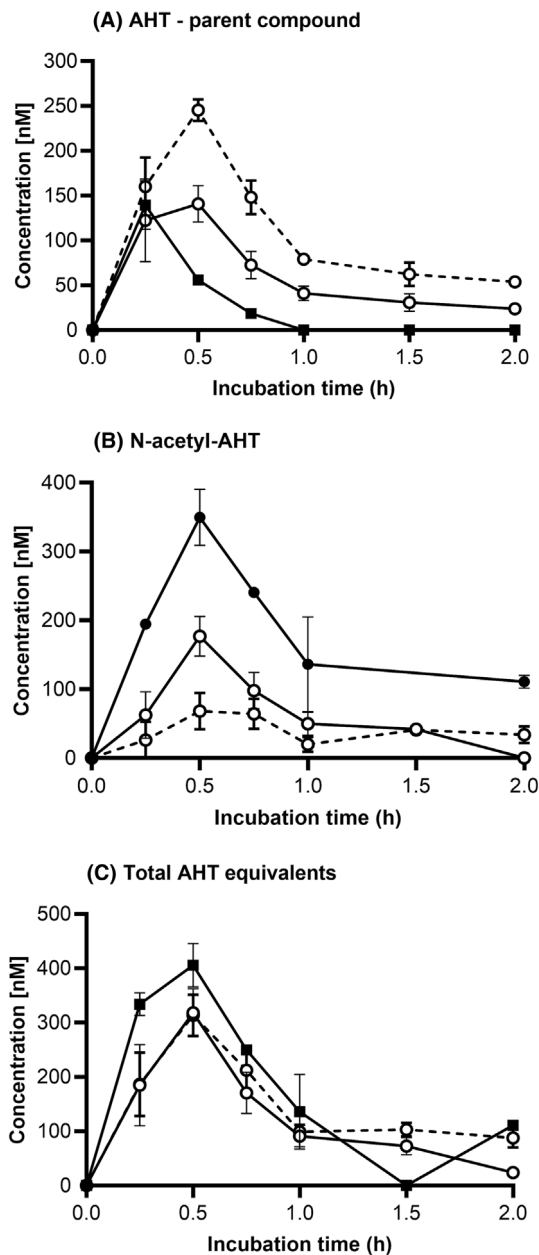
### 3.2 | Comparison of AHT permeation and metabolism in skin models in static incubations

Figure 2 shows the permeation of AHT and its *N*-acetyl-metabolite measured in static incubations with D17 and D21 SkinEthic™ models, compared with that in EpiDerm™ models previously reported by Tao et al. (2021). In EpiDerm™ models, the permeation of AHT into the medium after application peaked at 139 nM at 15 min (Figure 2A). After this time, the amount permeating decreased such that no more parent AHT was detected in the medium at the 1 h timepoint. In D17 and Day 21 SkinEthic™ models, the amount of AHT entering the medium over 2 h after application was higher compared to EpiDerm™



**FIGURE 1** H&E staining of sections of EpiDerm™, D17 SkinEthic™, EpiDermFT™ and PhenionFT™ models on Days 0 and 6 of incubation. Note that D17 SkinEthic™ models were only incubated in static cultures, whereas the other three models were incubated in the Chip2.

models. Higher concentrations were measured in the media of these model incubations at all timepoints after 15 min. The difference in the amount of AHT (parent compound) in the medium was due to the amount of AHT metabolised to *N*-acetyl-AHT, since the total concentration of parent AHT plus *N*-acetyl-AHT was similar (Figure 2C). This was also reflected by the results from incubations with EpiDerm™ models containing higher *N*-acetyl-AHT concentrations in the medium (111–350 nM) compared to the other two skin models (0–177 nM; Figure 2B). The applied AHT doses did not cause changes in the viability markers for any of the models tested (data not shown).



**FIGURE 2** Comparison of AHT permeation and metabolism in epidermal models cultured under static incubations. AHT was topically applied (dose equivalent to 2.5  $\mu$ M in the medium assuming 100% permeation) to D17 SkinEthic™ models (open circle symbols with a solid line), D21 SkinEthic™ models (open circle symbols with a dotted line) and EpiDerm™ models (closed square symbols). The concentration of (A) AHT, (B) *N*-acetyl-AHT and (C) total AHT equivalents entering the medium was measured at each timepoint. There was a 100% medium change at each timepoint. Values are mean  $\pm$  SEM,  $n = 3$  models. Values for the EpiDerm™ are from Tao et al. (2021).

The PhenionFT™ model was also evaluated in static incubations and compared to results using an epidermal model (in this case D17 SkinEthic™ models). The lag time of AHT permeation in PhenionFT™ was longer, and the maximum concentration of AHT (11  $\mu$ M) in the medium was significantly lower (Figure 3A). This was due to slower

permeation rate and metabolism to *N*-acetyl-AHT (95% of the AHT in the medium was present as the *N*-acetyl-metabolite) (Figure 3B). The total amount of AHT equivalents (Figure 3C) reaching the medium was much lower using PhenionFT™ models than D17 SkinEthic™ models.

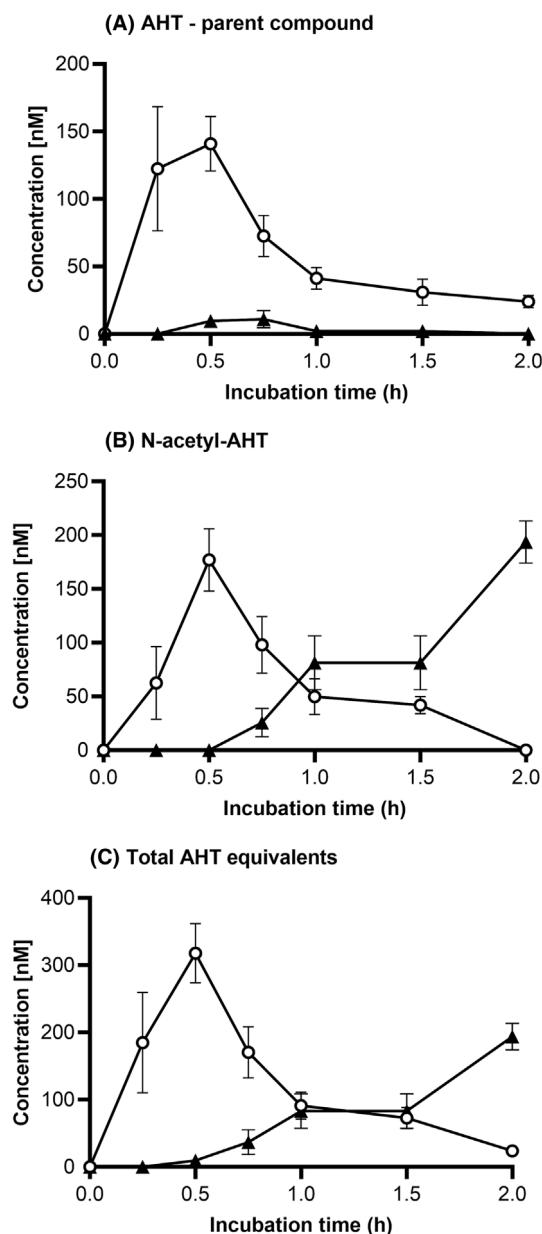


**FIGURE 3** Comparison of AHT permeation and metabolism in D17 SkinEthic™ (open circle symbols) and PhenionFT™ (closed triangle symbols) models cultured under static incubations. AHT was topically applied (dose equivalent to 2.5  $\mu$ M in the medium assuming 100% permeation). The concentration of (A) AHT, (B) *N*-acetyl-AHT and (C) total AHT equivalents entering the medium was measured at each timepoint. There was a 100% medium change at each timepoint. Values are mean  $\pm$  SEM,  $n = 3$  models.

### 3.3 | Chip2 incubations using PhenionFT™ models

None of the application scenarios of AHT or ethanol (solvent control) resulted in changes in the viability markers (Figure S1). There was a very low AHT concentration in the circuit after topical application compared to the same dose applied systemically (Figure 4). Less than 70 nM were detected in the circuit after 0.5 and 1 h, and concentrations were below the LOQ at all other timepoints (Figure 4A). Topical application decreased the AUC of AHT by 23- and 35-fold by applying AHT topically as a leave-on or rinse-off, respectively (Table 1).

The relative contribution of the *N*-acetylation pathway to AHT metabolism was markedly higher after topical leave-on application compared to systemic application of AHT (Figure 4B). The peak concentration of *N*-acetyl-AHT was  $713 \pm 23$  nM compared to  $377 \pm 41$  nM after systemic application, and the AUC of this metabolite was increased by 182% (Table 1). The peak concentration of AHT-O-sulphate was lower after leave-on topical compared to systemic application (Figure 4C) and its AUC was decreased (17% of the AUC after systemic application of this dose; Table 1). AHT-O-glucuronide formation (Figure 4D) was decreased (<LOD) after leave-on topical application. The concentration of the *N*-acetyl-AHT-O-sulphate was similar after systemic and leave-on topical application of AHT (Figure 4E).

The washing procedure performed 30 min after AHT application removed 43% of the applied dose, which correlated with the decrease in the AUC of the total AHT equivalents (31.5  $\mu$ M.h compared to 53.4  $\mu$ M.h after leave-on topical application; Table 1). The amount of AHT washed from the skin surface indicated that not all of the applied dose had been removed from the surface, because the concentration in the wash after six washes (207 nM) was still 10-fold higher than the LLOQ (25 nM). When AHT was washed from the skin surface of the PhenionFT™ models, the concentrations of *N*-acetyl-AHT and *N*-acetyl-AHT-O-sulphate were lower than when applied under leave-on conditions. When expressed as the percentage of the total metabolites, the amount of each metabolite after topical application was the same with and without the wash at 30 min (Table 1). Thus, the relative percentage of *N*-acetylation after rinse-off application (63% of the total metabolites) was also higher than that after systemic application (34% of the total metabolites).

## 4 | DISCUSSION

There are several RHE models available, with some exhibiting similar XME profiles to native human skin (Hewitt et al., 2013). Short-term 3D models have also been shown to mimic penetration (Abdallah et al., 2015; Hu et al., 2009) and metabolism properties of topically applied chemicals (Hu et al., 2009). A review of the use of RHEs (relating to their use in the pharmaceutical industry) summarises the advantages and disadvantages of these models (Mathes et al., 2014). Advantages of RHE models include a regular availability of the tissues, making experiment scheduling easier, as well as a reduction in inter-donor variability in results compared to native human skin. A

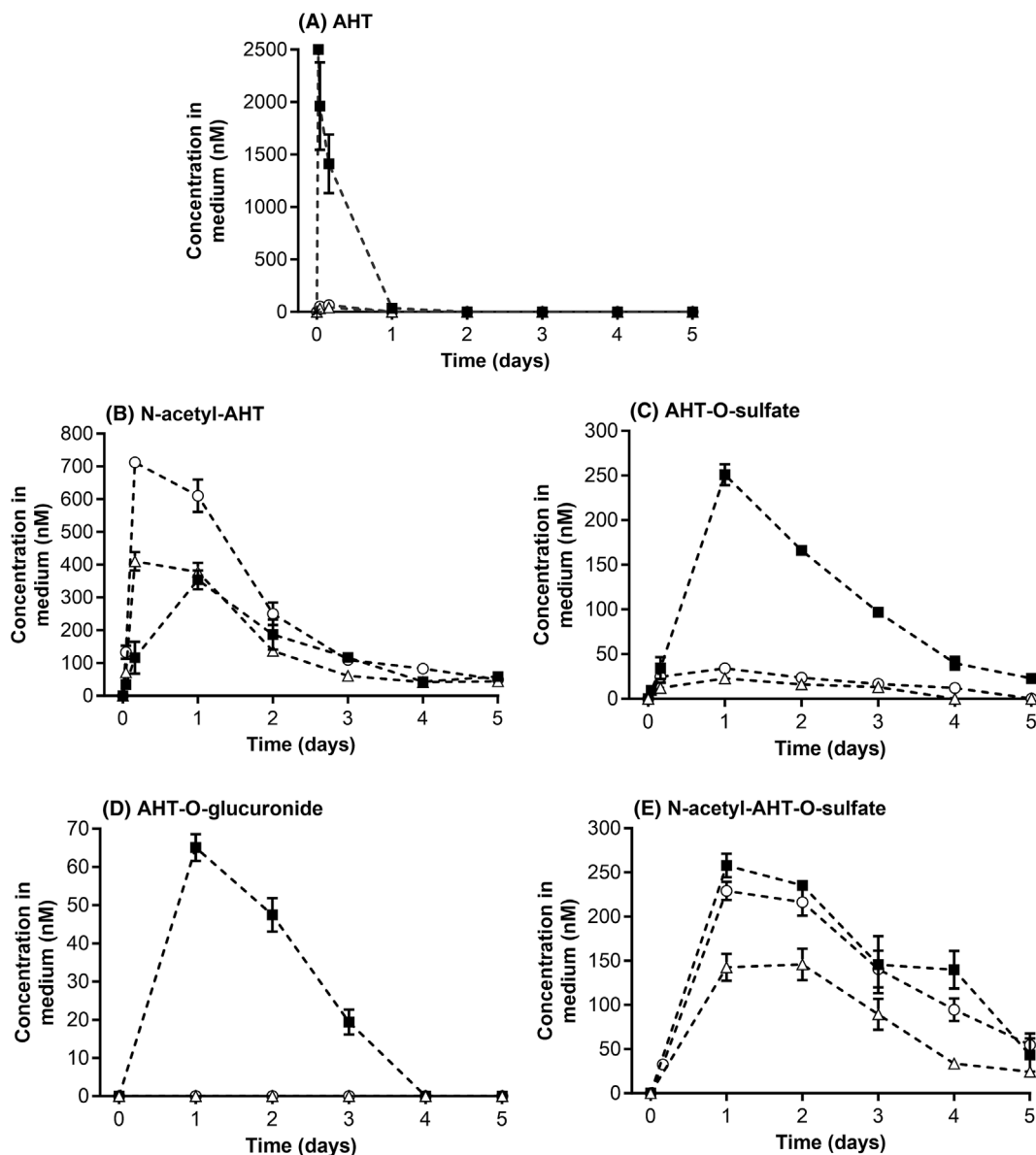


**FIGURE 4** Effect of the application route and rinse-off/leave-on conditions on the kinetics of AHT and its metabolites using PhenionFT™ models in the skin compartment of the Chip2. The concentrations of (A) AHT, (B) *N*-acetyl-AHT, (C) AHT-O-sulphate, (D) AHT-O-glucuronide and (E) *N*-acetyl-AHT-O-sulphate in the Chip2 after systemic (closed square symbols) and topical (leave-on = open circle symbols and rinse-off = open triangle symbols) application of 2.5  $\mu$ M AHT. Values are a mean of 3 circuits  $\pm$  SEM starting from 1 h after application. The data points are joined by dotted lines because they do not include the decrease in concentration due to the half medium change.

disadvantage of the RHE models is that penetration of chemicals may be higher through RHE models than through *ex vivo* skin (Ackermann et al., 2010); however, the integrity of all RHE and native human skin changes over time, such that the stratum corneum becomes thicker, thus changing the barrier function and penetration of chemicals.

This study investigated the suitability of different epidermal and FT skin models for use in the Chip2 model. Previous proof-of-concept studies were based on the relatively lipophilic model compounds, permethrin and hyperforin, in a Chip2 model using the epidermal model, EpiDerm™ (Kühnl et al., 2021). The penetration of these compounds is expected to be low, since a high logP is linked to low skin absorption (Bunge et al., 1995), which was reflected in the outcome of the

investigations (Kühnl et al., 2021). For such lipophilic compounds, the epidermal barrier limits the permeation and introduces *in vivo* relevant route-specific effects to the MPS compared to 2D models, for example, direct application to hepatocytes. However, AHT is a relatively hydrophilic compound (its logP is 0.795 [EPA]) and may be expected to rapidly permeate the relatively hydrophilic layers of the epidermis whereas it may permeate the lipophilic layers of the stratum corneum more slowly. In addition, it has been reported that the potential human systemic exposure to cosmetics ingredients may be overestimated due to the absence of metabolism in cadaver or frozen skin used in standard *in vitro* skin absorption assays (Nohynek et al., 2010). Cadaver skin might be several days old, resulting in low

**TABLE 1** AUC values of AHT and its quantified metabolites after systemic and leave-on and rinse-off topical application of 2.5  $\mu\text{M}$  to PhenionFT™ models. Values are a mean  $\pm$  SD of 3 circuits. A statistical difference ( $p < 0.05$ ) from values after systemic application is denoted with an asterisk (\*).

Parameter	Dosing scenario	AHT	N-acetyl-AHT	AHT-O-sulphate	AHT-O-glucuronide	N-acetyl-AHT-O-sulphate	Total AHT equivalents
AUC ( $\mu\text{M}\cdot\text{h}$ )	Systemic	20.9 $\pm$ 3.4	18.2 $\pm$ 1.6	13.5 $\pm$ 0.1	3.2 $\pm$ 0.4	19.2 $\pm$ 1.3	75.0 $\pm$ 3.6
	Topical leave-on	0.9 $\pm$ 0.1 *	33.1 $\pm$ 4.0 *	2.3 $\pm$ 0.6 *	0 $\pm$ 0 *	17.1 $\pm$ 1.1	53.4 $\pm$ 3.1
	Topical rinse-off	0.6 $\pm$ 0.2 *	19.4 $\pm$ 1.5	1.3 $\pm$ 0.2 *	0 $\pm$ 0 *	10.2 $\pm$ 0.6 *	31.5 $\pm$ 2.2
% Total metabolites	Systemic	NA	34 $\pm$ 3	25 $\pm$ 0	6 $\pm$ 1	36 $\pm$ 2	NA
	Topical leave-on	NA	63 $\pm$ 4	4 $\pm$ 1	0 $\pm$ 0	33 $\pm$ 3	NA
	Topical rinse-off	NA	63 $\pm$ 1	4 $\pm$ 0	0 $\pm$ 0	33 $\pm$ 1	NA

or no metabolic capacity, and the morphology of frozen skin may change due to freeze-thaw induced shrinking and stretching, which causes intercellular separation, thereby increasing the penetration of the test chemical. For this reason, some skin penetration studies use only fresh skin. Therefore, a model that more closely mimics the three layers, as well as the metabolic capacity of the skin, may be best suited for Chip2 experiments with this compound.

An important consideration when using skin models is they retain their morphology and metabolic function over time. With respect to the morphology, the stratum corneum layers of EpiDerm™ models thickened over time but contained large spaces, indicating the junctional complexes has been disrupted. While the epidermal layer was much thinner, it remained intact (and was still metabolically functional based on previous studies [Kühnl et al., 2021]). The stratum corneum of the SkinEthic™ model was also thicker over time, with some spaces between the layers but, unlike the EpiDerm™ model, the thickness of its epidermal layer was maintained, albeit with some vacuoles present. This may be due to its use in static incubations only, whereas the morphology of the other models was captured after 6 days in the Chip2 (and thus a constant flow of medium below the skin model). The morphology of the FT models was similar to native human skin upon delivery; however, by the end of the Chip2 incubation (Day 6), the dermis of the EpiDermFT™ models had almost disappeared, possibly due to the flow of medium below the insert. By contrast, the structure of the PhenionFT™ models appeared to be more stable under the Chip2 conditions, with little change in its morphology over the entire time course of the incubations. These observations were in accordance with their associated permeability and metabolism of AHT, with the slowest penetration and most extensive N-acetylation occurring in PhenionFT™ models compared to the epidermal models.

Our initial evaluation was made using static incubations to compare the penetration and metabolism of AHT in incubations with two epidermal models and the FT model, PhenionFT™. Incubations with the epidermal model, SkinEthic™, used 1 day after delivery (D17) indicated that the permeation of AHT was similar to that using the EpiDerm™ model. As the penetration through these models was much higher than in native human skin, it was hypothesised that a thicker stratum corneum would provide a better barrier to AHT; therefore, SkinEthic™ models were cultured for an additional 4 days before they

were tested for AHT permeability. However, the total permeation of AHT plus acetyl-AHT was the same in D17 and D21 SkinEthic™ models, indicating that this was not the case in these models. It is likely that although there were more layers of stratum corneum, they were not sufficiently compact to provide an effective barrier (as described above). Therefore, the barrier properties do not solely depend on the dimension of a skin model's stratum corneum but also other important features, such as a non-disrupted structure with relevant lipids and intracellular tight junctions. When PhenionFT™ models were used in static incubations, the penetration of total AHT equivalents was much slower than in the epidermal models, and much lower concentrations were detected in the medium (10 nM compared to 141 nM using SkinEthic™ models) only after 0.5 h (compared to after 15 min using SkinEthic™ models). The penetration of AHT across PhenionFT™ models continued to increase over 2 h, whereas in SkinEthic™ models almost all AHT had penetrated into the medium by this time. The difference in penetration of AHT indicates that PhenionFT™ models represented a higher barrier to AHT than epidermal models, due to it being a thicker tissue with a well-structured stratum corneum similar to native skin. Moreover, this permeation profile better reflected the permeation of this hair dye through native human skin (Goebel et al., 2009). This model also extensively metabolised AHT to N-acetyl-AHT as it passed through the skin layers. All epidermal models were also able to metabolise AHT, with the EpiDerm™ model exhibiting higher N-acetylation than the SkinEthic™ models. The lower metabolism of AHT in older (D21) SkinEthic™ models compared to EpiDerm™ models indicated that a thicker stratum corneum was at the expense of fewer viable keratinocytes and lower metabolic activity.

The PhenionFT™ was evaluated for use in the skin-liver Chip2 to determine whether it could mimic the route-dependent differences in the kinetics of AHT and its metabolites observed in in vivo studies. As observed in previous studies with reconstructed skin models, topical application of AHT altered the ratio of metabolites, with an increase in N-acetyl-AHT from 34% after systemic application to 63% after topical application (either leave-on or rinse-off). Likewise, the ratio of AHT-sulphate was decreased (from 25% to 4% of the total metabolites). As observed in the previous study, the ratio of N-acetyl-AHT-O-sulphate was similar after systemic and leave-on or rinse-off topical

applications of AHT. This finding was attributed to AHT sulfation occurring prior to *N*-acetylation and that *N*-acetylation of AHT precludes a further sulfation step (Tao et al., 2021).

The observation that the metabolism of AHT by the liver organoids was dependent on the skin model and hence, the medium used, was also noted in the current study with the PhenionFT™ model. The relative contribution of *N*-acetylation, glucuronidation and sulfation of AHT after systemic application in Chip2 experiments using PhenionFT™ models was 34%, 25% and 6% of the total metabolites, respectively, compared to 13%, 39% and 12% in EpiDermFT™ models. This was attributed to the different medium causing a change in enzyme activities in the HepaRG cells (Tao et al., 2021). This difference did not affect the evaluation of the first-pass *N*-acetylation since the route comparisons were run in the same medium. This difference in metabolism is unlikely to be due to changes in skin metabolism because the effect was observed after systemic application, whereby the contribution of skin metabolism was much lower than that of liver (because the medium is only in contact with the underside of the skin models). In addition, the skin models did not metabolize AHT to AHT-glucuronidate or AHT-sulphate metabolites, which were both impacted by the medium used. On the one hand, this underlines the high reproducibility of the model to identify effects in a specific condition but, on the other hand, implies a need to consolidate culture conditions towards a 'best practice' to resemble the *in vivo* situation or how to approach a specific assessment goal.

The kinetics of AHT and its metabolites in the Chip2 demonstrated previously using the EpiDerm™ and EpiDermFT™ models were compared with those using the PhenionFT™ model. With the exception of the Day 1 timepoint, the kinetics of total AHT equivalents (i.e., AHT plus all four quantified metabolites) were similar after systemic application to Chip2 circuits containing EpiDerm™ and EpiDermFT™ or PhenionFT™ models (Figure 5A). This indicates, that while the ratio of metabolites produced differed, the overall metabolic clearance was independent of the skin model and medium used. After leave-on topical application, the kinetics of total AHT equivalents were comparable in EpiDerm™ and EpiDermFT™ models (Figure 5B), indicating that the penetration combined with the overall rate of metabolic clearance of AHT was the same. This similarity between the epidermal and FT models is unlikely to be due to the observed loss of the dermis in EpiDermFT™ models (resulting in a poorer barrier), since the static incubations indicated that AHT absorption was complete within a few hours of application, whereas the loss of the dermis observed on Day 5 is likely to take days to occur and was unlikely to be affected at this early timepoint. The peak concentration of AHT in the Chip2 circuit was marginally higher in experiments with EpiDermFT™ models compared to experiments with EpiDerm™ models; however, this may be due to the different rates of subsequent metabolism by the liver organoids rather than to differences in the skin models. In accordance with the preliminary experiments using static incubations, the application of AHT to PhenionFT™ models in the Chip2 markedly decreased the overall exposure to total AHT equivalents (Figure 5B) and AHT (Figure 5C). This indicates that the PhenionFT™ model exhibited higher barrier properties to this hydrophilic chemical than the EpiDerm™ and EpiDermFT™ models.

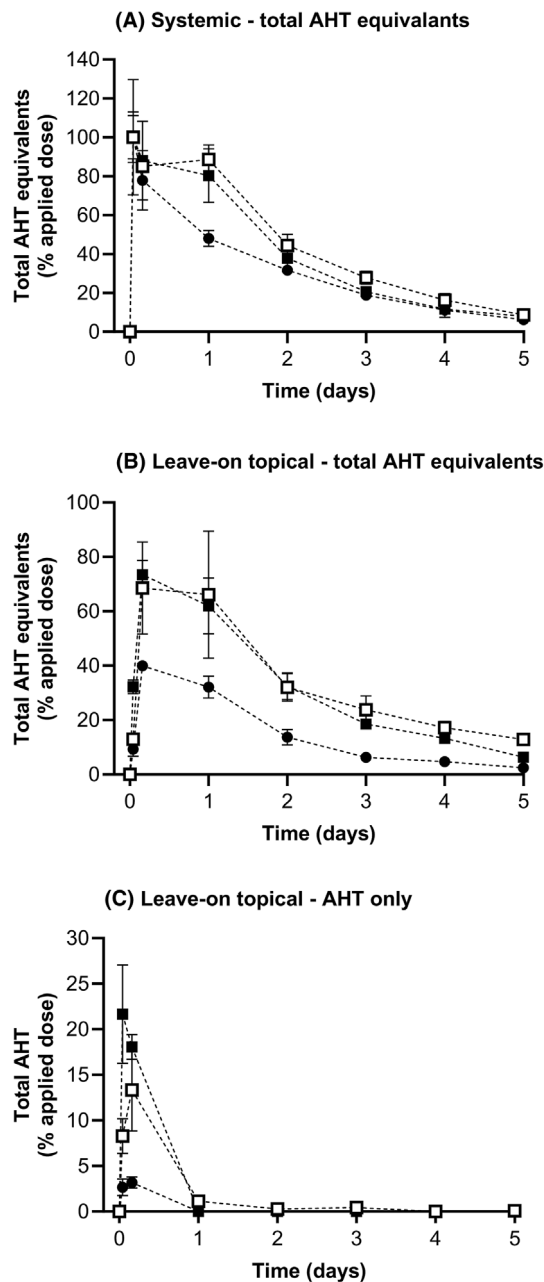


**FIGURE 5** Comparison of systemic exposure to AHT after application to different skin models in the skin compartment of the Chip2. Concentration of (A) total AHT equivalents after systemic application, (B) total AHT equivalents and (C) AHT only, after leave-on topical application to EpiDerm™ (open square symbols), EpiDermFT™ (closed square symbols) and PhenionFT™ (closed circle symbols) models. Values are expressed as the concentration of total AHT equivalents or AHT as a percentage of the actual applied dose (since these differed slightly between experiments). Values are a mean of 3–5 circuits  $\pm$  SEM starting from 1 h after application. The data points are joined by dotted lines since they do not include the decrease in concentration due to the half medium change. Values for the EpiDerm™ and EpiDermFT™ are from Tao et al. (2021).

MPS are promising models that enable more *in vivo*-relevant evaluations. For cosmetic ingredients, the skin-liver Chip2 model can be used to evaluate the kinetics of chemicals applied under consumer

relevant exposures. For example, a skin care lotion is best evaluated under leave-on conditions, whereas a hair dye is ideally evaluated using a 30-min exposure. It was possible to evaluate the effect of rinsing the skin surface on the AHT kinetics in the investigations using EpiDermFT™ and PhenionFT™ models, because they have sufficiently large surface areas to enable the procedure. Smaller skin models are more technically challenging to wash without damaging the barrier. As with previous studies, rinsing the PhenionFT™ models after 30 min markedly decreased the exposure of AHT and its metabolites. This model also appeared to be particularly robust, with very little changes in its structure noted on Day 5, even after topical application and subsequent washing.

In conclusion, the dynamic nature of the skin-liver Chip2 model enables a more realistic estimation of systemic exposure and kinetics of topically applied test chemicals over 5 days, without the need for further extrapolation or modelling to the in vivo situation. We have demonstrated that both epidermal and FT skin models can mimic the first-pass metabolism of AHT in the skin, which was previously demonstrated in in vivo studies. Additional chemicals and application scenarios over longer durations will need to be tested to make a more comprehensive evaluation of different skin models for use in the Chip2. However, based on AHT only, this study highlights the flexibility of the Chip2 to incorporate different skin models, thereby providing multiple options for experimental approaches.

## ACKNOWLEDGEMENTS

This work was funded by the Cosmetics Europe Long Range Science Strategy programme.

## CONFLICT OF INTEREST STATEMENT

The authors have no conflict of interest.

## DATA AVAILABILITY STATEMENT

The data that support the findings of this study are available from the corresponding author upon reasonable request.

## ORCID

Nicola J. Hewitt  <https://orcid.org/0000-0002-1045-0748>

## REFERENCES

- Abdallah, M. A., Pawar, G., & Harrad, S. (2015). Evaluation of in vitro vs. in vivo methods for assessment of dermal absorption of organic flame retardants: A review. *Environment International*, 74, 13–22. <https://doi.org/10.1016/j.envint.2014.09.012>
- Ackermann, K., Borgia, S. L., Korting, H. C., Mewes, K. R., & Schäfer-Korting, M. (2010). The Phenion full-thickness skin model for percutaneous absorption testing. *Skin Pharmacology and Physiology*, 23(2), 105–112. <https://doi.org/10.1159/000265681>
- Alexander-White, C., Bury, D., Cronin, M., Dent, M., Hack, E., Hewitt, N. J., Kenna, G., Naciff, J., Ouedraogo, G., Schepky, A., Mahony, C., & Europe, C. (2022). A 10-step framework for use of read-across (RAX) in next generation risk assessment (NGRA) for cosmetics safety assessment. *Regulatory Toxicology and Pharmacology*, 129, 105094. <https://doi.org/10.1016/j.yrtph.2021.105094>
- Bunge, A. L., Cleek, R. L., & Vecchia, B. E. (1995). A new method for estimating dermal absorption from chemical exposure. 3. Compared with steady-state methods for prediction and data analysis. *Pharmaceutical Research*, 12(7), 972–982. <https://doi.org/10.1023/a:1016298012408>
- Dent, M. P., Vaillancourt, E., Thomas, R. S., Carmichael, P. L., Ouedraogo, G., Kojima, H., Barroso, J., Ansell, J., Barton-Maclaren, T. S., Bennekou, S. H., Boekelheide, K., Ezendam, J., Field, J., Fitzpatrick, S., Hatao, M., Kreiling, R., Lorencini, M., Mahony, C., Montemayor, B., ... Yang, C. (2021). Paving the way for application of next generation risk assessment to safety decision-making for cosmetic ingredients. *Regulatory Toxicology and Pharmacology*, 125, 105026. <https://doi.org/10.1016/j.yrtph.2021.105026>
- Desprez, B., Dent, M., Keller, D., Klaric, M., Ouedraogo, G., Cubberley, R., Duplan, H., Eilstein, J., Ellison, C., Grégoire, S., Hewitt, N. J., Jacques-Jamin, C., Lange, D., Roe, A., Rothe, H., Blaauboer, B. J., Schepky, A., & Mahony, C. (2018). A strategy for systemic toxicity assessment based on non-animal approaches: The Cosmetics Europe long range science strategy programme. *Toxicology in Vitro*, 50, 137–146. <https://doi.org/10.1016/j.tiv.2018.02.017>
- EU. (2003). EC-Directive 2003/15/EC of the European Parliament and of the Council of 27 February 2003 amending Council Directive 76/768/EEC on the approximation of the laws of the member states relating to cosmetic products. Off. J. 26, L66.
- Géniès, C., Jacques-Jamin, C., Duplan, H., Rothe, H., Ellison, C., Cubberley, R., Schepky, A., Lange, D., Klaric, M., Hewitt, N. J., Grégoire, S., Arbey, E., Fabre, A., & Eilstein, J. (2020). Comparison of the metabolism of 10 cosmetics-relevant chemicals in EpiSkin™ S9 subcellular fractions and in vitro human skin explants. *Journal of Applied Toxicology*, 40(2), 313–326. <https://doi.org/10.1002/jat.3905>
- Géniès, C., Jamin, E. L., Debrauwer, L., Zalko, D., Person, E. N., Eilstein, J., Grégoire, S., Schepky, A., Lange, D., Ellison, C., Roe, A., Salhi, S., Cubberley, R., Hewitt, N. J., Rothe, H., Klaric, M., Duplan, H., & Jacques-Jamin, C. (2019). Comparison of the metabolism of 10 chemicals in human and pig skin explants. *Journal of Applied Toxicology*, 39(2), 385–397. <https://doi.org/10.1002/jat.3730>
- Goebel, C., Hewitt, N. J., Kunze, G., Wenker, M., Hein, D. W., Beck, H., & Skare, J. (2009). Skin metabolism of aminophenols: Human keratinocytes as a suitable in vitro model to qualitatively predict the dermal transformation of 4-amino-2-hydroxytoluene in vivo. *Toxicology and Applied Pharmacology*, 235(1), 114–123. <https://doi.org/10.1016/j.taap.2008.11.014>
- Hewitt, N. J., Edwards, R. J., Fritsche, E., Goebel, C., Aebly, P., Scheel, J., Reisinger, K., Ouedraogo, G., Duche, D., Eilstein, J., Latil, A., Kenny, J., Moore, C., Kuehn, J., Barroso, J., Fautz, R., & Pfuhler, S. (2013). Use of human in vitro skin models for accurate and ethical risk assessment: Metabolic considerations. *Toxicological Sciences: an Official Journal of the Society of Toxicology*, 133(2), 209–217. <https://doi.org/10.1093/toxsci/kft080>
- Hu, T., Bailey, R. E., Morrall, S. W., Aardema, M. J., Stanley, L. A., & Skare, J. A. (2009). Dermal penetration and metabolism of p-aminophenol and p-phenylenediamine: Application of the EpiDerm human reconstructed epidermis model. *Toxicology Letters*, 188(2), 119–129. <https://doi.org/10.1016/j.toxlet.2009.03.019>
- Kühnl, J., Tao, T. P., Brandmair, K., Gerlach, S., Rings, T., Müller-Vieira, U., Przbilla, J., Genies, C., Jaques-Jamin, C., Schepky, A., Marx, U., Hewitt, N. J., & Maschmeyer, I. (2021). Characterization of application scenario-dependent pharmacokinetics and pharmacodynamic properties of permethrin and hyperforin in a dynamic skin and liver multi-organ-chip model. *Toxicology*, 448, 152637. <https://doi.org/10.1016/j.tox.2020.152637>
- Lee, H. R., & Sung, J. H. (2022). Multiorgan-on-a-chip for realization of gut-skin axis. *Biotechnology and Bioengineering*, 119(9), 2590–2601. <https://doi.org/10.1002/bit.28164>
- Li, H., Reynolds, J., Sorrell, I., Sheffield, D., Pendlington, R., Cubberley, R., & Nicol, B. (2022). PBK modelling of topical application and

- characterisation of the uncertainty of C (max) estimate: A case study approach. *Toxicology and Applied Pharmacology*, 442, 115992. <https://doi.org/10.1016/j.taap.2022.115992>
- Mathes, S. H., Ruffner, H., & Graf-Hausner, U. (2014). The use of skin models in drug development. *Advanced Drug Delivery Reviews*, 69–70, 81–102. <https://doi.org/10.1016/j.addr.2013.12.006>
- Moxon, T. E., Li, H., Lee, M. Y., Piechota, P., Nicol, B., Pickles, J., Pendlington, R., Sorrell, I., & Baltazar, M. T. (2020). Application of physiologically based kinetic (PBK) modelling in the next generation risk assessment of dermally applied consumer products. *Toxicology in Vitro*, 63, 104746. <https://doi.org/10.1016/j.tiv.2019.104746>
- Najjar, A., Schepky, A., Krueger, C. T., Dent, M., Cable, S., Li, H., Grégoire, S., Roussel, L., Noel-Voisin, A., Hewitt, N. J., & Cardamone, E. (2022). Use of physiologically-based kinetics modelling to reliably predict internal concentrations of the UV filter, Homosalate, after repeated Oral and topical application. *Frontiers in Pharmacology*, 12, 802514. <https://doi.org/10.3389/fphar.2021.802514>
- Nohynek, G. J., Antignac, E., Re, T., & Toutain, H. (2010). Safety assessment of personal care products/cosmetics and their ingredients. *Toxicology and Applied Pharmacology*, 243(2), 239–259. <https://doi.org/10.1016/j.taap.2009.12.001>
- Ouedraogo, G., Alexander-White, C., Bury, D., Clewell, H. J. 3rd, Cronin, M., Cull, T., Dent, M., Desprez, B., Detroyer, A., Ellison, C., Giammanco, S., Hack, E., Hewitt, N. J., Kenna, G., Klaric, M., Kreiling, R., Lester, C., Mahony, C., Mombelli, E., ... Cosmetics Europe (2022). Read-across and new approach methodologies applied in a 10-step framework for cosmetics safety assessment - a case study with parabens. *Regulatory Toxicology and Pharmacology*, 132, 105161. <https://doi.org/10.1016/j.yrtph.2022.105161>
- Tao, T.-P., Brandmair, K., Gerlach, S., Przibilla, J., Génies, C., Jacques-Jamin, C., Schepky, A., Marx, U., Hewitt, N. J., Maschmeyer, I., & Kühnl, J. (2021). Demonstration of the first-pass metabolism in the skin of the hair dye, 4-amino-2-hydroxytoluene, using the Chip2 skin-liver microphysiological model. *Journal of Applied Toxicology: JAT*, 41(10), 1553–1567. <https://doi.org/10.1002/jat.4146>
- Tao, T.-P., Maschmeyer, I., LeCluyse, E. L., Rogers, E., Brandmair, K., Gerlach, S., Przibilla, J., Kern, F., Genies, C., Jacques, C., Najjar, A., Schepky, A., Marx, U., Kühnl, J., & Hewitt, N. J. (2023). Development of a microphysiological skin-liver-thyroid Chip3 model and its application to evaluate the effects on thyroid hormones of topically applied cosmetic ingredients under consumer-relevant conditions. *Frontiers in Pharmacology*, 14, 1076254. <https://doi.org/10.3389/fphar.2023.1076254>
- Tavares, R. S. N., Tao, T. P., Maschmeyer, I., Maria-Engler, S. S., Schäfer-Korting, M., Winter, A., Zoschke, C., Lauster, R., Marx, U., & Gaspar, L. R. (2020). Toxicity of topically applied drugs beyond skin irritation: Static skin model vs. two organs-on-a-chip. *International Journal of Pharmaceutics*, 589, 119788. <https://doi.org/10.1016/j.ijpharm.2020.119788>

## SUPPORTING INFORMATION

Additional supporting information can be found online in the Supporting Information section at the end of this article.

**How to cite this article:** Brandmair, K., Tao, T.-P., Gerlach, S., Przibilla, J., Schepky, A., Marx, U., Hewitt, N. J., Kühnl, J., & Maschmeyer, I. (2023). Suitability of different reconstructed human skin models in the skin and liver Chip2 microphysiological model to investigate the kinetics and first-pass skin metabolism of the hair dye, 4-amino-2-hydroxytoluene. *Journal of Applied Toxicology*, 1–11. <https://doi.org/10.1002/jat.4542>